Integrated Computer-Aided Engineering Journal, 2005

Obstacle Detection using a Time-of-Flight Range Camera for Automated Guided Vehicle Safety and Navigation

Roger Bostelman

ph. 301-975-3426, fax 301-921-6165

Tsai Hong

ph. 301-975-3444, fax 301-990-9688

Raj Madhavan

ph. 301-975-2865, fax 301-990-9688

Intelligent Systems Division

Manufacturing Engineering Laboratory

National Institute of Standards and Technology

100 Bureau Drive, MS 8230, Gaithersburg, MD 20899,

ABSTRACT

The performance evaluation of an obstacle detection and segmentation algorithm for Automated Guided Vehicle (AGV) navigation in factory-like environments using a 3D real-time range camera is the subject of this paper. Our approach has been tested successfully on British safety standard recommended object sizes and materials placed on the vehicle path. The segmented (mapped) obstacles are then verified using absolute measurements obtained using a relatively accurate 2D scanning laser rangefinder. Sensor mounting and sensor modulation issues will also be described through representative data sets.

INTRODUCTION

Background

Obstacle detection and mapping are crucial for autonomous indoor driving. This is especially true for Automated Guided Vehicle (AGV) navigation in factory-like environments where safety of personnel and that of the AGV itself are of utmost importance. This paper describes the performance of an obstacle detection and segmentation algorithm using a 3D real-time range camera.

The 3D range camera tested is a Time-Of-Flight (TOF) device [8] and is capable of simultaneously producing intensity images and range information of targets in indoor environments. This range camera has great potential for obstacle detection in industrial applications as it will be relatively inexpensive as compared to similar sensors and can deliver range and intensity images at a rate of 30 Hz with an active range of 7.5 m while incorporating no moving parts, such as a spinning mirror, unlike many off-the-shelf laser sensors.

Since obstacle detection plays a basic function for autonomous driving, there has been much research on many different types of sensors, such as sonar [12], color/gray level cameras [2], FLIR (Forward Looking InfraRed) cameras [11], and stereo cameras [10], [1], [13], [6]. Most of the vision approaches are not applicable to indoor scenes due to lack of texture in the environment (e.g., plain walls, low lighting, etc.). Other researchers have proposed LADAR (Laser Detection And Ranging) sensors for detecting obstacles [4], [3], [5]. However, two-dimensional data produced by line-scanning LADAR, are not suitable for the 3D world of

factory environments and other complex volumes, and necessitates moving the sensor during operation.

Our proposed approach to obstacle detection uses a low cost, 3D, real-time, range camera, called the CSEM SwissRanger II[1]. First, we calibrate the camera with respect to the AGV so that we can convert the range values to 3D point clouds in the AGV coordinate frame. Second, we segment those objects which have high intensity and whose elevation values are above the floor of the operating environment on the AGV path. The segmented 3D points of the obstacles are then projected and accumulated into the floor surface-plane. The algorithm utilizes the intensity and 3D structure of range data from the camera and does not rely on the texture of the environment. The segmented (mapped) obstacles are verified using absolute measurements obtained using a relatively accurate 2D scanning laser rangefinder (range and angular resolution to 15 mm (0.6 in) and 0.004 rad (0.25°)). Our approach has been tested successfully on cotton covered objects of approximately British safety standard recommended sizes placed on the vehicle path. For this paper, the AGV remained stationary as the measurements were collected.

Safety Standards

A proposed change to the American Society of Mechanical Engineers (ASME) B56.5 standard [14][2] allows non-contact safety sensors as opposed to contact sensors such as bumpers on AGVs. Prior to this change, the B56.5 standard defined an AGV bumper as a “mechanically actuated

[1] Commercial equipment and materials are identified in this paper in order to adequately specify certain procedures. Such identification does no imply recommendation or endorsement by the National Institute of Standards and Technology, nor does it imply that the materials or equipment identified are necessarily the best available for the purpose.

[2] Authors note: the proposed change has not been accepted by ASME to date.

device, which when depressed, causes the vehicle to stop." The proposed change reflects the standard committee's recommendations to use proven non-contact sensing devices in place of (or along with) mechanical AGV bumpers. The allowance of non-contact safety sensors on AGVs opens new areas of vehicle control generally supporting the safety notion of not only stopping the vehicle but, also slowing the vehicle around high-risk objects, such as humans. For example, should the vehicle sensors detect walls, shelving, posts, etc., the vehicle may continue to move at higher speeds than if the sensors detect what could be human arms or legs. With the proposed B56.5 standard change and with state-of-the-art non-contact safety sensors, vehicles can be shorter in length, excluding mechanical bumpers, allowing shorter turning radii and potentially move faster as objects can be detected well before the vehicle is close to an object.

Ideally, the U.S. standard can be modified even further and made more similar to the British EN1525 safety standard requirements [15]. The British safety standard of industrial, driverless trucks requires that: "(a) sensors shall operate at least over the full width of the vehicle and load in every direction of travel, (b) sensors shall generate a signal enabling the vehicle to be stopped by the braking system under specified floor conditions before contact between the rigid parts of the vehicle and/or load and a person, (c) sensors shall detect parts of a person's body as close as possible to the floor but at least the "test apparatus shall be detected", (d) The activation of such sensors shall not cause injury to persons, and (e) reflective characteristics of test apparatus for personnel detection means which work without physical contact shall be representative of human clothing." We anticipate the work described in this paper and the continuing research efforts to lay the groundwork towards further modification to the US safety standards for AGVs in factory-like environments where perhaps specific object sizes and shapes are used to specify detection-

sensor requirements. Furthering the US safety standard will also provide support toward a unified, global safety standard for AGVs and other driverless vehicles.

The paper is structured as follows: the beginning section describes the concept of obstacle detection and segmentation including the 3D range camera, algorithm, and a modulation issue using range camera images. The next section provides the experimental setup and results when the proposed algorithm is employed for detection and segmentation of British standard size and material-covered test apparatus. Next, a section provides even further discussion beyond the typical indoor factory environment application and indicates future research areas that are under investigation including sensor mounting and outdoor daylight tests and results. A summary and conclusion follows with acknowledgments and a reference list.

OBSTACLE DETECTION AND SEGMENTATION

3D Range Camera

In this section, we describe an algorithm to detect and segment obstacles in the path of the AGV using a solid-state Time-Of-Flight (TOF) range camera. The 3D range camera shown in Figure 1 is a compact, robust and cost effective solid state device capable of producing 3D images in real-time. The camera measures 14.5 cm x 4 cm x 3 cm (5.7 in x 1.6 in x 1.2 in), has a field of view of 0.7 rad (42°) horizontal x 0.8 rad (46°) vertical, and is capable of producing range images of 160 pixels x 124 pixels. Additional specifications are listed in Table 1. For a brief overview of the characteristics and operating principles of the camera, see [9]. Approximately sized British standard test obstacles, shown in Figure 2, were placed on the travel path.

The British EN1525 safety standard specifies that horizontal test pieces used to test sensors shall be 200 mm (7.9 in) diameter x 600 mm (23.6 in) long lying perpendicular to the vehicle path. Vertical test pieces shall be 70 mm (2.8 in) diameter and 400 mm (15.7 in) tall completely within the vehicle path.

Algorithm Details

The obstacle detection algorithm processes the range data and determines not only the obstacle range, but also segments the obstacles from their environment and places them in the maps in the world model. The algorithm combines intensity and range images from the range camera to detect the obstacles and estimate the distance to the obstacles.

We first calibrate the camera with respect to the AGV so that we can convert the range values to 3D points in the AGV coordinate frame. Next, we segment those objects which have high intensity and whose elevation values are above the floor of the operating environment on the AGV path. The segmented 3D points of the obstacles are then projected and accumulated into the floor surface-plane. The algorithm utilizes the intensity and 3D structure of range data from the camera and does not rely on the texture of the environment. The segmented (mapped) obstacles are verified using absolute measurements obtained using a 2D scanning laser rangefinder with a range uncertainty of 3 cm (1.2 in).

Specifically, the steps of the algorithm are illustrated in Figure 3 for a sample image from the range camera:

1) a patch of data with high intensity values (i.e., greater than half of the average brightness of intensity value returned from the camera) in the front of the robot is used to fit a plane for

estimating the floor surface as shown in Figure 3(a). In our experiments, the average intensity value returned from the camera is a robust threshold value to measure the goodness of range return.

However, we believe that a learning algorithm should be implemented to learn what is the threshold value to optimize the best range returns on the floor or other environment areas.

2) the left and right edges of the 3D robot paths (the sensors and robot were stationary) are projected to the range and intensity images such that only obstacles on the path (i.e., the hallway) that can be considered as shown in Figure 3(b). The path is chosen and defined by the planner in our 4D/RCS (4-Dimensional, Real-time Control System) [16].

3) all the intensity pixels inside of the left and right edges are used to hypothesize the potential obstacle. If the intensity value of the pixel is greater than half of the average of the intensity in the image, then the pixel is considered as a potential obstacle as shown in Figure 3(c).

4) each potential obstacle pixel in the range image is used to find the distance to the floor plane when the distance to the floor is greater than a user-defined threshold as shown in Figure 3(d). The threshold is dependent on the traversability (ground clearance) of the robot and sensor placement with respect to the floor.

Potential obstacles in the world model can be accumulated as the AGV moves. Figure 4 shows an obstacle map representation that is part of the world model – overhead map of obstacles. The obstacles map is shown at 10 cm grid resolution. Nearly all the apparatus obstacles are found, although at the cost of false positives from the reflected objects (reflectors mounted to the walls at further distances). To improve the reliability of obstacle detection, the obstacles in the map

and information obtained from an added color camera may be temporally integrated. Such integration has proven to be a very useful cue for obstacle detection [8].

Modulation Issue

An issue with this particular range camera is the modulation of returned data at approximately 7.5 m. Within the range of approximately 7.5 m, the camera accurately senses (to within 3 mm) the range to objects. Beyond 7.5 m, the camera continues to sense objects although it places the object data within the modulation of 7.5 m. For example, an object detected at 11 m would be placed in the returned data at a range (11 m – 7.5 m) = 3.5 m (see Figure 5).

To eliminate the modulation issue, a lower emitted light modulation frequency (ELMF) below the typical 20 MHz can be used to establish a longer, yet lower accuracy (as stated by the manufacturer) range modulation and could be used to compare with the 7.5 m range modulated range data. The compared data within the two modulation frequencies can then be used to mask objects detected beyond the 7.5 m range. Also, similar to how humans have and use peripheral vision, these longer-range objects created by a higher ELMF setting could be placed in the world model for additional (though higher uncertainty) environmental information. A human peripheral vision provides excellent motion detection [7], the higher ELMF setting could produce low relative accuracy, yet larger range and volume (see Figure 6) motion detection of obstacles. While the disadvantage here is producing lower relative range uncertainty, the advantage for vehicle control is that decisions can be made much earlier to react to potential obstacles farther away, even if their exact range is unknown.

EXPERIMENTAL SETUP AND RESULTS

The experiments were conducted under two scenarios as stated within the British Standard:

- A test apparatus with a diameter of 200 mm (7.9 in) and a length of 600 mm (23.6 in) placed at right angles on the path of the AGV. The actuating force on this test apparatus shall not exceed 750 N.
- A test apparatus with a diameter of 70 mm (2.8 in) and a height of 400 mm (15.7 in) set vertically within the path of the AGV. The actuating force on this test apparatus shall not exceed 250 N.

Figures 2(a) and (b) show the experimental apparatus for the two aforementioned scenarios. The center of the range camera lens was centered to focus on approximately the centroid of the apparatus for all measurements. The scanning laser rangefinder had no measurable (using a ruler) vertical offset from the range camera, and was offset 250 mm horizontally and to the left of the camera as viewed from the camera to the test apparatus. The range camera was used to detect a known test apparatus mounted on a stand moved to different locations with respect to the range camera.

The obstacle detection and segmentation algorithm was tested on two British standard test apparatus as described in [15], placed at 0.5 meter to 7.5 m distances to the sensor, and was evaluated against ground truth. A line scanning laser rangefinder, shown in Figure 7, mounted beside the range camera, was used to simultaneously verify the distance to the test apparatus for each data set and served as ground truth. The rangefinder produces 401 data points over a 100° semi-circular region in front of the robot.

Table 2 shows the performance of the range camera for measuring the distance to the test apparatus placed at several distances from the range camera. As can be seen, the uncertainty (mean of multiple scans) of the range decreases as the distance to the apparatus placed in front of the range camera is increased.

In Figure 8, the test apparatus (shown in Figure 2 (a) and with corresponding results shown in Figures 4 and 5) was placed at a distance of 2.5 m from the range camera. Each object in the test apparatus was clearly detected even though the range camera was also sensitive to the reflectors on the wall of the hallway. The resultant intensity, range, and segmented images are shown in Figures 8(a), (b) and (c), respectively. Note that although the intensity and range images in Figures 8 (a) and (b) show reflections on the floor, the segmented algorithm with results shown in Figure 8 (c) removes these by removing objects below the floor plane. The ground truth provided by the scanning laser rangefinder is shown in Figure 8(d) and has been rotated to show a top-down view.

In Figure 9, (shown in Figure 2 (b) and with corresponding results shown in Figure 3) the test apparatus is a mannequin leg placed on the floor with an approximate diameter of 200 mm and a length of 600 mm. This test apparatus is more challenging for the algorithm because the entire object is close to the floor. As can be seen, the legs are detected, but at the cost of detecting reflectors mounted on the walls at further distances than the apparatus. Since some reflectors (see Figure 9(c)) are at a distance of more than 7.5 m, they are modulated by the non-ambiguity distance range of the camera. Again, this deficiency can be eliminated by using two different

modulation frequencies (such as 10 MHz and 20 MHz) where the detected objects would be coarsely represented at a more appropriate distance. The control algorithm can then intelligently delete them. The ground truth, single-line scan LADAR, with results shown in Figure 9 (d), shows not only the relatively parallel mannequin leg surface to the sensor (center to right), but also an irregularity on the left as the LADAR detected a non-parallel leg surface to the sensor. The closest parallel surface to the sensor and shown in the image center and right were used as the reference range in our experiment.

FURTHER RESEARCH

Sensor Mount

Critical to the sensor itself is the mounting configuration of the sensor to enable detection of objects within the vehicle path. Although there are no specific guidelines within the above US standard for sensor mounts, it does suggest that the sensor be "fail-safe" and regarding bumpers, they "shall activate from a force applied parallel to the floor." Fix-mounting the sensor with its view in the direction of vehicle travel seems ideal where for example, a sensor that was mounted on perhaps a rotary head might possibly not detect an approaching obstacle outside the rotated FOV. A range camera rigidly mounted on the vehicle and near the floor is also ideal where reflected data off the floor is less likely to detect the floor as an object. However, taller vehicles may need to view higher volumes as overhead objects may be within the vehicle path. Similarly, AGVs typically have sensors that detect objects such as human feet to the side of the vehicle. Non-contact safety sensors must therefore, wrap their FOV around the vehicle using mirrors or other devices or simply duplicate sensors to gain larger FOVs to incorporate these potentially hazardous regions. Figure 10 shows one possible configuration of 3D range cameras mounting

locations to sense both in front of the vehicle and also the sides. This concept could have potential detection issues that may be simply solved by timing the light emission from each camera to consecutively, as opposed to simultaneously, enable light emission and detection from the sensor. For example, camera 3 can theoretically be turned on, collect data, and turn off before camera 4 senses emission from camera 3. The cycle can be fast enough to stop the vehicle in an emergency. NIST algorithms allow frame rates at 30 Hz providing relatively fast data for vehicle controllers to react appropriately to sensed data. Moreover, pairs of cameras 1, 2 and 5, 6 could be combined from independent camera FOVs into a dual camera FOV. Side cameras could be added as well.

Data was collected with two 3D cameras and is shown in Figure 11. The Figure shows a photograph of a scene using the same vertical post test apparatus as shown in Figure 2(b) and placed at approximately 0.8 m (30 in) above the floor between a table (left) and a desk (right) with the 3D camera at approximately 1 m (39 in) above the floor. The two images were merged in real-time such that the left and right 3D camera images can be viewed as a single image. The processed image was colored slightly differently so the operator could distinguish between the two camera responses. Clearly, objects within the scene, including a small crane model on the left, can be determined to be objects. Ideally, as graphically shown in Figure 10, additional cameras can be joined together to provide an even larger field of view surrounding the vehicle.

Outdoor daylight tests and results

In an effort to move beyond typical indoor AGV applications toward increased robot navigational intelligence, the sensor was taken outdoors. Moving vehicles from indoors to

outdoors opens up a wide area of applications where safety sensors are necessary and require alternative sensing capability. For example, AGV applications could include material handling from indoors to outdoors to a staging area or into another building such as in the shipbuilding industry. This industry typically has long, narrow shipyards along water potentially supporting the need for autonomous vehicles carrying a variety of part sizes and shapes and navigating around people, clutter, buildings, and other vehicles. Safety of people and equipment is a large concern and will require sensors capable of sensing through all weather and light conditions to which the vehicle is exposed, as well as lighting from indoor or outdoor shade to full sun no matter what time of day the vehicle is functional.

Although the 3D range camera manufacturer has stated that the camera is currently only reliable when used during indoor lighting conditions, the authors felt that a minimal inclusion in this paper is relevant to current AGV applications and provides the reader with a broader scope of future sensor applications. Replacing the LEDs on the camera with laser diodes is possible and could improve the bright lighting condition challenges. In our experiment with the LED camera, it was taken outdoors during daylight hours although the conditions were cloudy (full overcast) and the robot supporting the sensor was positioned in the shade beneath leaf-covered tree branches. The experiment begins to address outdoor lighting and object detection issues, such as sensing objects that are potentially recognizable, without fully exhausting all outdoor light conditions.

Figure 12 shows a photo of a large tree trunk and branches along with 3D range information about the tree with respect to the camera positioned about 2.5 m away. The rear, right branch

also shows a clear difference in range data toward 3.5 m where it measures, using a ruler, approximately 1 m behind the front, center branch. Objects behind the tree are approximately a minimum of 14 m away and the ground incrementally approaches in range from 1 m to 2.5 m between the camera and the tree, as the range data shows. Notice the similarity of the tree in the photo to the range and segmented data, where range information about the tree is uncertain to within several centimeters. This uncertainty is left somewhat vague as the tree has a very irregular surface and shape. The range response was consistent since the manufacturer states that the camera has range uncertainty to within 3 mm.

Similarly, Figure 13 shows a photo of the corner of a building along with the 3D range information about the corner with respect to the camera positioned about 2.5 m away. In this case however, the sun was shining brighter on the left side while more shaded on the right. Similar to the tree data, the corner range data was uncertain to within a few centimeters. Although the sharp corner is indecipherable perhaps due to the angle of reflection being approximately 45°, there is definite range response from the camera showing that a large object is in front of the robot regardless of the bright/shaded light conditions. Some small detail can also be picked out of the building corner range data as the right side brick, from the corner to 43 cm away from the corner, is recessed by 1.5 cm and the recess is visible in the data as a vertical line. However, an algorithm to determine this line from the overall corner data may be difficult to design.

SUMMARY AND CONCLUSIONS

An obstacle detection and segmentation algorithm for Automated Guided Vehicle (AGV) navigation in factory-like environments using a novel 3D range camera was described in this paper. The range camera is highly attractive for obstacle detection in industrial applications as it will be relatively cheap and can deliver range and intensity images in real-time with the vehicle control. The performance of the algorithm was evaluated by comparing it with ground truth provided by a single-line scanning laser rangefinder.

A concept for sensor mounting was also described, with corresponding data collected and represented for combining two or more sensors for a larger sensor FOV. Also, a sensor modulation issue was described with a suggested remedy to allow objects beyond the 7.5 m modulation distance to be known or eliminated from the data.

We envisage the extension of the work detailed in this paper in the following areas:

- We believe that the range camera can be used for moving obstacle detection from a moving AGV for indoor applications. The detection of moving obstacles in the factory floor is a next critical step for AGV navigation in such dynamic environments. Additionally, this sensor can be combined with a color camera for detecting and tracking obstacles over long distances.
- We also believe that the range camera discussed in this paper holds good potential to be used in outdoor environments where, perhaps laser diodes could replace the LEDs for intense ambient light conditions. Towards this, we have taken and analyzed some outdoor data and the preliminary results show good promise in using this sensor for outdoor forest environments, in other areas that are shaded, and in night conditions. Some prospective applications include mapping factory environments (“lights-out”) manufacturing inside and

outside during night (dark) hours, and even for use in space due to its light weight and compactness.

ACKNOWLEDGEMENTS

The authors would like to thank Peter Russo, student worker from the University of Maryland, for his contribution of dual, 3D camera sensor processing. Also, the authors thank John Gibbons, Transbotics Corp. for suggesting the study of wrap-around mounted sensors.

REFERENCES

[1] P. Batavia and S. Singh. Obstacle Detection Using Adaptive Color Segmentation and Color Stereo Homography. In Proc. of the IEEE Intl. Conf. on Robotics and Automation, May 2001.

[2] M. Bertozzi, A. Broggi, A. Fascioli, and P. Lombardi. Artificial Vision in Road Vehicles. In Proc. of the 28th IEEE Industrial Electronics Society Annual Conf., 2002.

[3] T. Chang, T-H. Hong, S. Legowik, and M. Abrams. Concealment and Obstacle Detection for Autonomouos Driving. In Proc. of the Intl. Association of Science and Technology for Development - Robotics and Application, 1999.

[4] A. Ewald and V. Willhoeft. Laser Scanners for Obstacle Detection in Automotive Application. In Proc. of the Intell. Vehicles Symp., 2000.

[5] J. Hancock, M. Hebert, and C. Thorpe. Laser Intensity-based Obstacle Detection. In Proc. of the IEEE/RSJ Intl. Conf. on Intelligent Robots and Systems, 1998.

[6] M. Hariti, Y. Ruichek, and A. Koukam. A Voting Stereo Matching Method for Real-Time Obstacle Detection. In Proc. of the IEEE Intl. Conf. on Robotics and Automation, 2003.

[7] Hecht, Eugene, Optics, Schaum's Outline Series, McGraw-Hill ,1975

[8] T-H. Hong, T. Chang, C. Rasmussen, and M. Shneier. Feature Detection and Tracking for Mobile Robots Using a Combination of Ladar and Color Images. In Proc. of the IEEE Intl. Conf. on Robotics and Automation, May 2002.

[9] T. Oggier, M. Lehmann, R. Kaufmann, M. Schweizer, M. Richter, P. Metzler, G. Lang, F. Lustenberger, and N. Blanc. An All-solidstate Optical Range Camera for 3D Real-time Imaging with Subcentimeter Depth Resolution. In Proc. of the SPIE Conf. on Optical System Design, September 2003.

[10] C. Olson, L. Matthies, H. Schoppers, and M. Maimone. Robust Stereo Ego-motion for Long Distance Navigation. In Proc. of the IEEE Intl. Conf. on Computer Vision and Pattern Recognition, 2000.

[11] K. Owens and L. Matthies. Passive Night Vision Sensor Comparison for Unmanned Ground Vehicle Stereo Vision Navigation . In Proc. of the IEEE Intl. Conf. on Robotics and Automation.

[12] N. Sgouros, G. Papakonstantinous, and P. Tsanakas. Localized Qualitative Navigation for Indoor Environments. In Proc. of the IEEE Intl. Conf. on Robotics and Automation, 1996.

[13] R. Williamson and C. Thorpe. A Trinocular Stereo System for Highway Obstacle Detection. In Proc. of the IEEE Intl. Conf. on Robotics and Automation, 1999.

[14] American Society of Mechanical Engineers' Safety Standard for Guided Industrial Vehicle and Automated Functions of Manned Industrial Vehicle. Technical Report ASME B56.5, 1993.

[15] British Standard Safety of Industrial Trucks - Driverless Trucks and their Systems. Technical Report BS EN 1525, 1998.

[16] J. Albus, "4-D/RCS Version Reference Model Architecture for Unmanned Ground

Vehicles”, Proceedings of the 2000 International Conference on Robotic and Automation, 2000.

Table 1 – CSEM SwissRanger 2 Camera Specifications [9]

Parameter	*Specification*
Number of LEDs	48 for short distance version, up to 3 x 48 for long distance range
Supply Voltage	12 V
Modulation frequency	20 Mhz
Non-ambiguous distance range	7.5 m
Measured demodulation depth	40 %
Interface	USB 2.0 (USB 1.1 possible)
Number of pixels	160 x 124
Pixel size	39.2 µm x 54.8 µm
Pixel field	6.27 mm (160 pixels) x 6.80 mm (128 pixels)

Table 2 Quantitative Comparison of Performance

Nominal Obstacle Distance (cm)	*3D Range Camera Mean (cm)*	*2D Rangefinder Mean (cm)*
64	64.1	64.7
111	111.0	111.3
160	161.4	160.7
210	204.0	210.0
259	249.5	259.1
310	284.7	310.2

Figure Captions

Figure 1 - The TOF 3D range image camera. The camera simultaneously generates intensity images and range information of targets in its field-of view at a rate of 30 Hz with an active range of 7.5 m.

Figure 2 - Experimental setup (a) vertical test apparatus where the center object most closely matches the British standard size test piece measuring 65 mm dia. x 400 mm long. The remaining vertical objects are all thinner. (b) horizontal test apparatus (mannequin leg) measuring a segment approximately tapered from 80 mm to 160 mm dia. x 600 mm long including the leg from the ankle to the thigh. Both (a) and (b) objects are covered in cloth as also specified in the standard. See Experimental Setup and Results section for further details.

Figure 3 - Obstacle segmentation algorithm illustration. Obstacle detection, the obstacles in the map and information obtained from an added color camera may be temporally integrated. Such integration has proven to be a very useful cue for obstacle detection [8].

Figure 4 - Obstacle map.

Figure 5 – Segmented obstacles (left) and obstacle map (right) but, due to range modulation, obstacles detected beyond 7.5 m max. camera range are placed within the 7.5 m range.

Figure 6 – Graphic depicting range information (left) versus potential range information (right) with an alternative emitted light modulation frequency.

Figure 7 - Experimental setup of the AGV, the scanning laser rangefinder, and the range camera.

Figure 8 - Results of the obstacle detection and segmentation algorithm for the experimental setup shown in Figure 2(a). The resultant intensity, range, and segmented images are shown in (a), (b) and (c), respectively. The ground truth provided by the scanning laser rangefinder is shown in (d) and has been rotated to show a top-down view.

Figure 9 - Results of the obstacle detection and segmentation algorithm for the experimental setup shown in Figure 2(b). The resultant intensity, range, and segmented images are shown in (a), (b) and (c), respectively. The ground truth provided by the scanning laser rangefinder is shown in (d) and has been rotated to show a top-down view.

Figure 10 - Graphic showing one possible configuration of 3D range cameras mounting locations to detect not only in front of the vehicle but, also to the sides

Figure 11 – (a) Photo of a test scene, (b) 3D range camera image from two, merged cameras, and (c) segmented objects. The left and right cameras processed data are shown with different colors to allow the operator to easily understand each camera's data.

Figure 12 (a) shows a photo of a tree and (b) shows 3D range information and (c) shows segmented data about the distance of the tree with respect to the camera.

Figure 13 (a) shows a photo of the corner of a building and (b) shows 3D range information and (c) shows segmented data about the distance of the corner with respect to the camera. Note how the corner is not distinctly defined, except for the vertical inset brick line on the right, although clearly a large object (corner) is evident in the data.

Figure 1

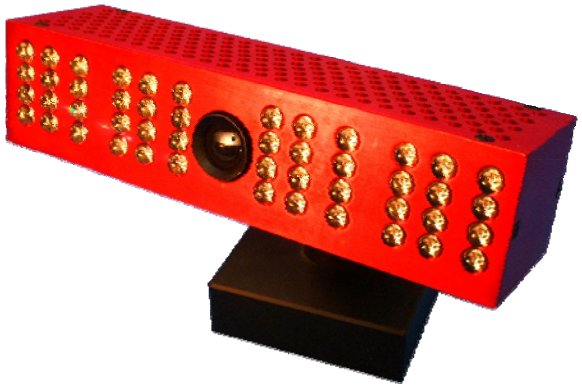

Figure 2

(a)

(b)

Figure 3

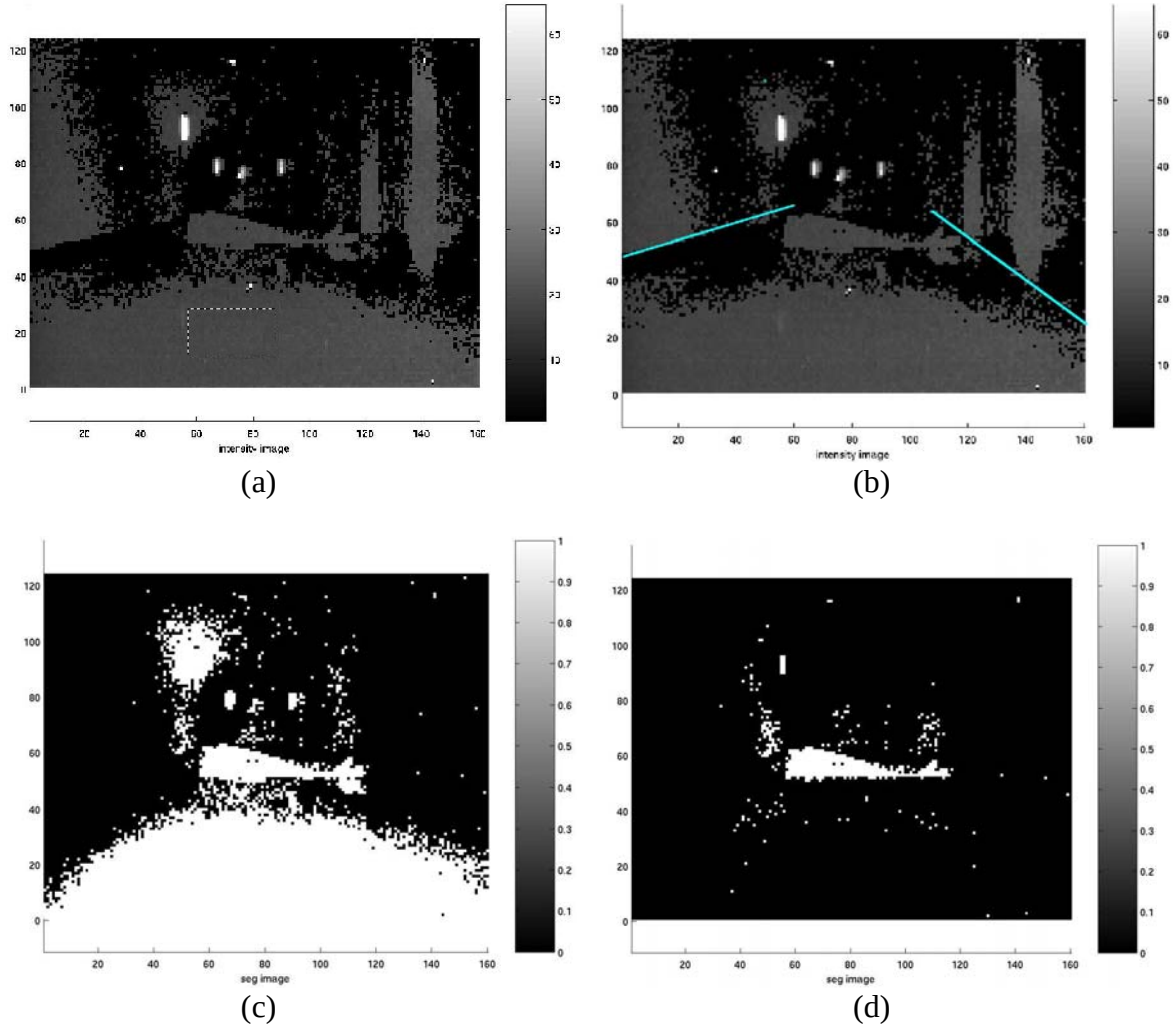

Figure 4

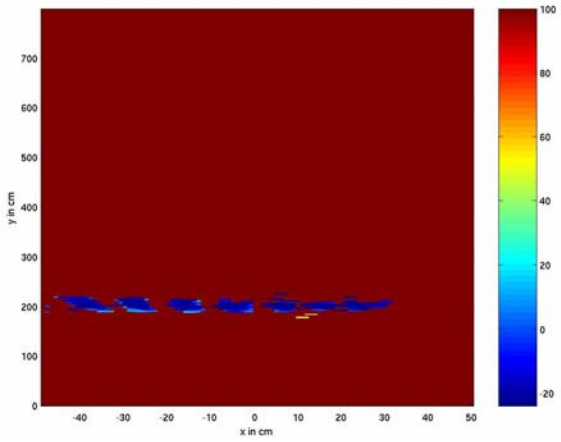
y in cm
x in cm
0
100
200
300
400
500
600
700
-40
-30
-20
-10
0
10
20
30
40
50
100
80
60
40
20
0
-20

Figure 5

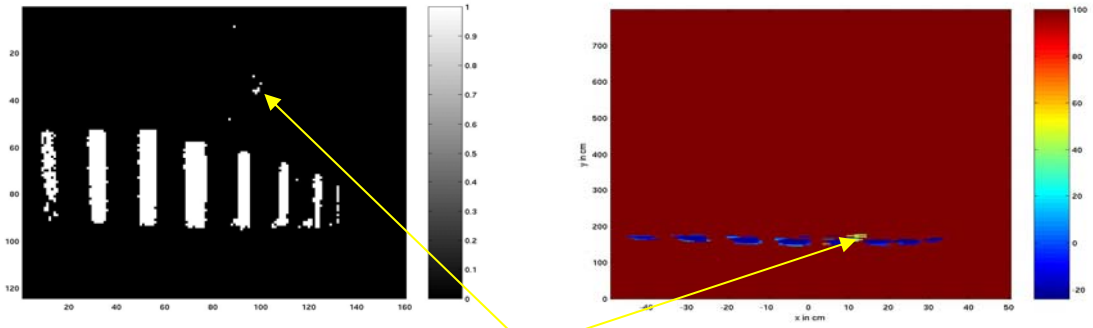

11 m distance to left-detected object incorrectly placed at ~3.5 m in right object map range

Figure 6

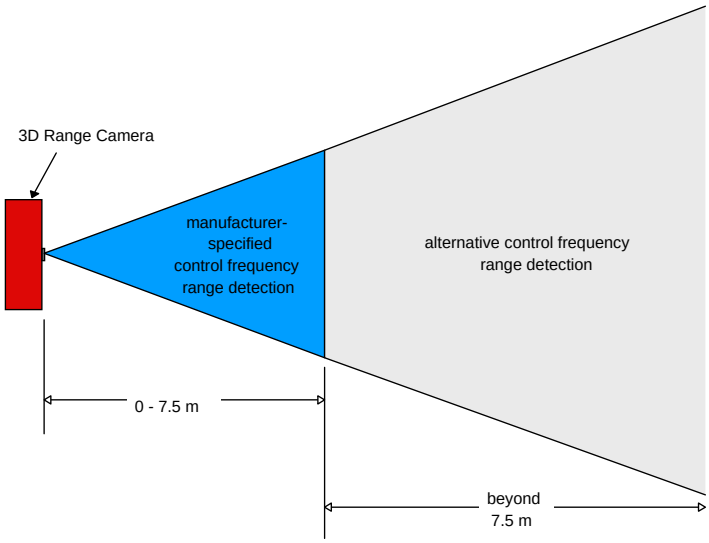
3D Range Camera
manufacturer-specified control frequency range detection
alternative control frequency range detection
0 - 7.5 m
beyond 7.5 m

Figure 7

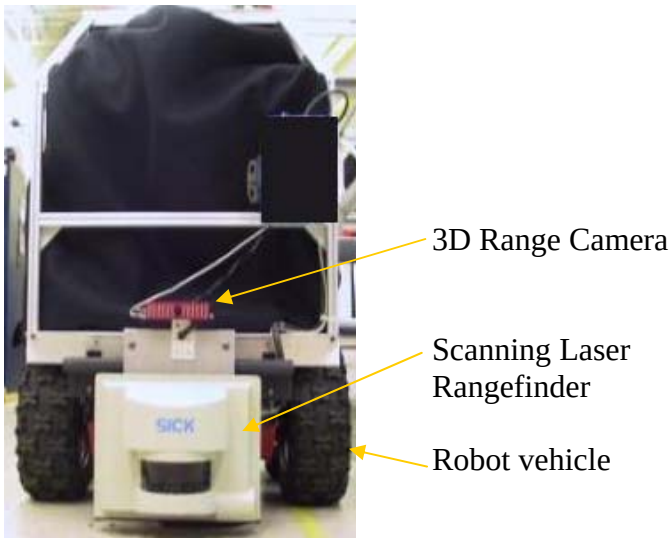
3D Range Camera
Scanning Laser Rangefinder
Robot vehicle
SICK

Figure 8

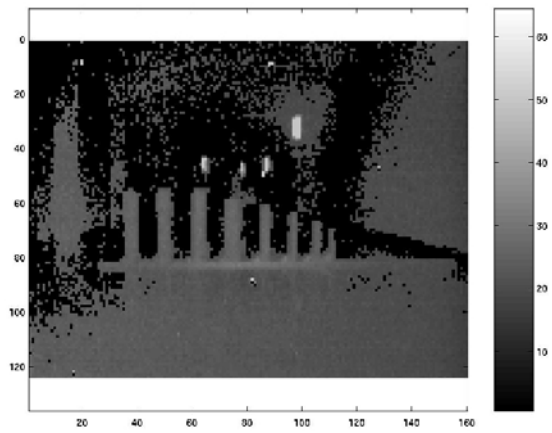

(a)

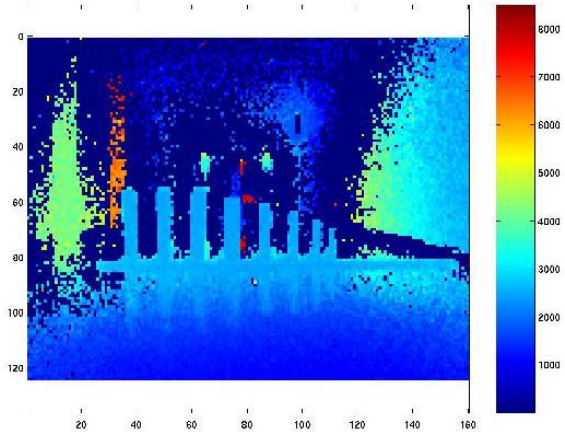

(b)

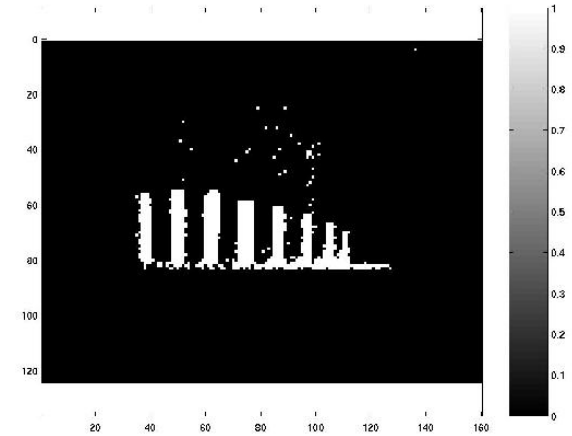

(c)

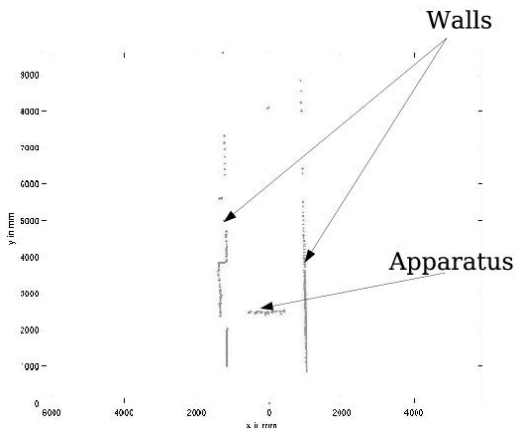

(d)

Figure 9

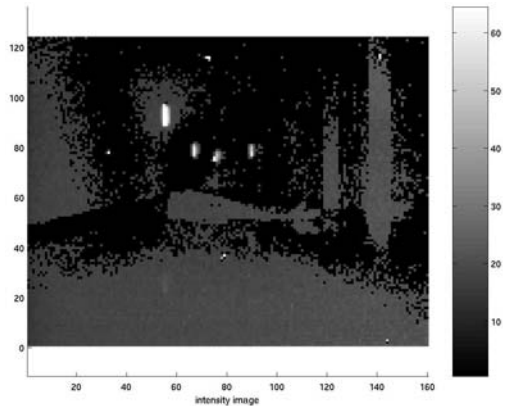

(a)

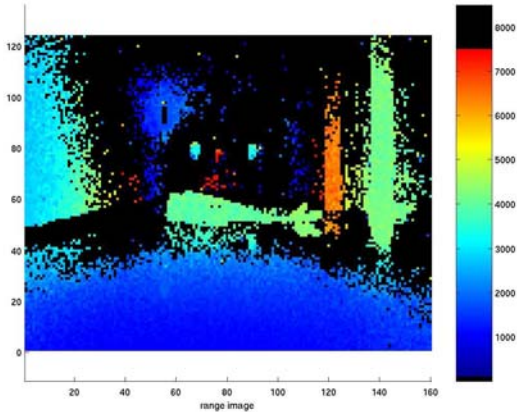

(b)

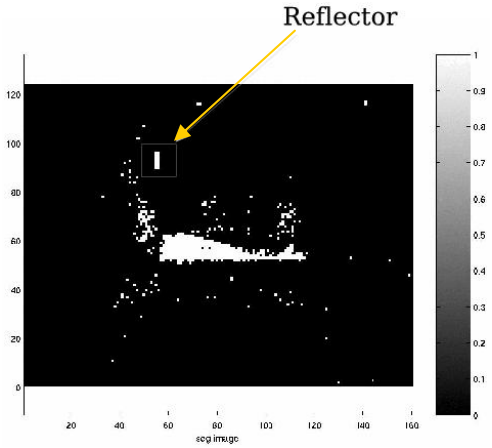

(c)

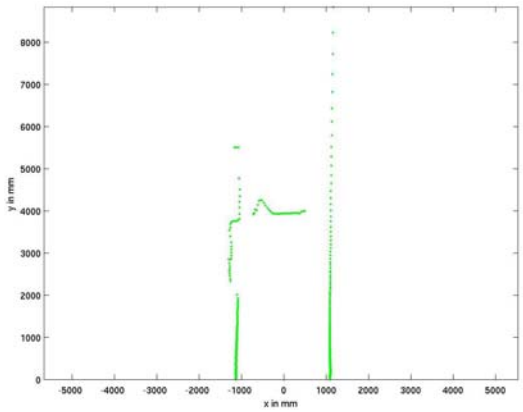

(d)

Figure 10

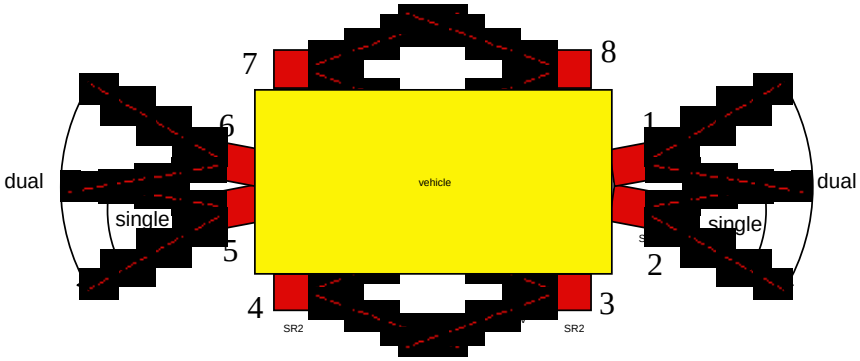

Figure 11

(a)

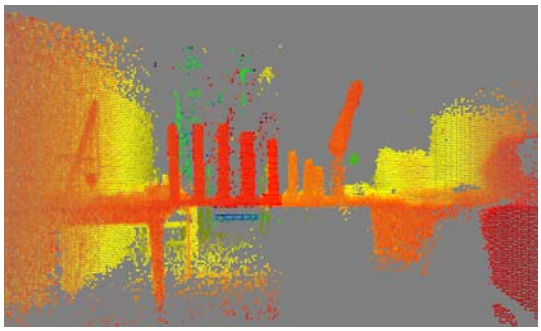

(b)

(c)

Figure 12

(a)

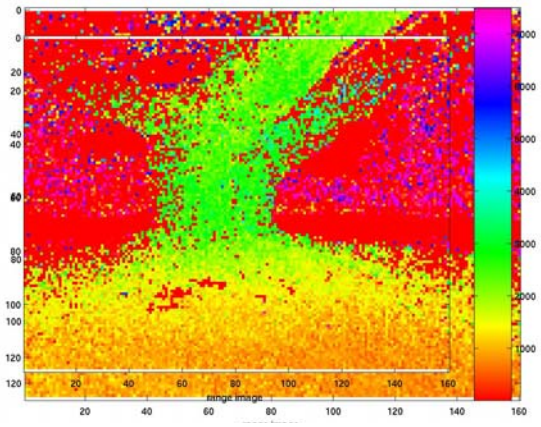

(b)

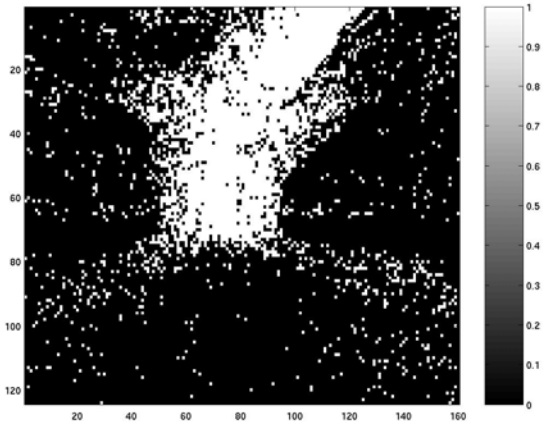

(c)

Figure 13